Article

High Pulse Energy, Narrow Linewidth 6.45 μm from an Optical Parametric Oscillator in BaGa₄Se₇ Crystal

Yu Shen [1,2,†], **Ning Wen** [1,3,†], **Chunxiao Li** [1,3], **Nan Zong** [1,2,*], **Jiyong Yao** [1,*], **Jinquan Chang** [1,3], **Ya Wen** [4], **Feng Yang** [1,2], **Wenlong Li** [5], **Hongwei Gao** [1,2], **Yong Bo** [1,2], **Qinjun Peng** [1,2] and **Dafu Cui** [1,2]

1   Key Lab of Functional Crystal and Laser Technology, Technical Institute of Physics and Chemistry, Chinese Academy of Sciences, Beijing 100190, China; shenyu@mail.ipc.ac.cn (Y.S.); wenning17@mails.ucas.ac.cn (N.W.); lichunxiao18@mails.ucas.ac.cn (C.L.); changjinquan19@mails.ucas.ac.cn (J.C.); yang12345yang@163.com (F.Y.); gaohongwei@mail.ipc.ac.cn (H.G.); boyong@tsinghua.org.cn (Y.B.); pengqinjun@mail.ipc.ac.cn (Q.P.); dfcui40@mail.ipc.ac.cn (D.C.)
2   Key Lab of Solid-State Laser, Technical Institute of Physics and Chemistry, Chinese Academy of Sciences, Beijing 100190, China
3   University of Chinese Academy of Sciences, Beijing 100190, China
4   Institute of Optical Physics & Engineering Technology, Qilu Zhongke, Jinan 250103, China; winvene@163.com
5   Chengdu Dien Photoelectric Technology Company Limited (DIEN TECH Co. Ltd.), Chengdu 610100, China; liwenlong@dientech.com
*   Correspondence: zongnan@mail.ipc.ac.cn (N.Z.); jyao@mail.ipc.ac.cn (J.Y.); Tel.: +86-010-82543471 (N.Z.); +86-010-82543474 (J.Y.)
†   These authors contributed equally to this work.

Abstract: This paper presents a high pulse energy, narrow linewidth, mid-infrared (MIR) laser at 6.45 μm, based on a BaGa₄Se₇ (BGSe) crystal optical parametric oscillator (OPO) pumped by 1.064 μm laser. The maximum pulse energy at 6.45 μm was up to 1.23 mJ, with a pulse width of 24.3 ns and repetition rate of 10 Hz, corresponding to an optical–optical conversion efficiency of 2.1%, from pump light 1.064 μm to idler light 6.45 μm. The idler light linewidth was about 6.8 nm. Meanwhile, we accurately calculated the OPO phase-matching condition at BGSe crystal pumped by 1.064 μm laser, and a numerical simulation system was performed to analyze the input–output characteristics at 6.45 μm, as well as the effect of crystal length on the conversion efficiency. Good agreement was found between measurement and simulation. To the best of our knowledge, this is the highest pulse energy at 6.45 μm, with the narrowest linewidth for any all-solid-state MIR ns laser in BGSe-OPO pumped by simple 1.064 μm oscillator. This simple and compact 6.45 μm OPO system, with high pulse energy and narrow linewidth, can meet the requirements for tissue cutting and improve tissue ablation accuracy.

Keywords: optical parametric oscillator (OPO); BaGa₄Se₇ crystal; 6.45 μm mid-infrared (MIR) laser

1. Introduction

Tissue ablation in human, for example, brains and eyes, requires the highest precision in the target tissues, reducing collateral damage to surrounding tissues, as far as possible. The viability of the remaining tissues is crucial to assess the effectiveness of ablation. Particularity, the mid-infrared (MIR) laser at 6.45 μm has tremendous potential as a high-precision surgical tool, as it offers minor collateral damage and a rapid ablation rate [1]. The penetration depth by 6.45 μm laser amounts to several μm, which approximates the single cell thickness and approaches the optimal value [2]. Especially, it is useful for ablation in ocular, neural, and dermal tissues [3]. Therefore, the development of the MIR laser at 6.45 μm has become a perennial hot topic. Four ways are commonly used to obtain 6.45 μm laser, including free electron lasers (FELs), gas Raman lasers, strontium vapor lasers, and solid-state lasers, based on nonlinear optical (NLO) frequency conversion techniques [1,2,4,5]. However, the high cost and bulky structure of FELs limit their extensive

application. Short operating life and tedious maintenance also hinder the development of gas Raman and strontium vapor lasers. In view of the precise and compact requirements of their application, solid-state lasers based on NLO frequency conversion techniques are an attractive means to generate high-energy MIR waves, such as optical parametric generation (OPG), the optical parametric amplifier (OPA), and the optical parametric oscillator (OPO). Among these general methods, OPO based on MIR crystals with good nonlinear properties and accessible pump lasers is a promising candidate for generating high-performance, long-wave MIR sources. At present, a variety of promising NLO crystals, which can be pumped by 1 μm laser to obtain a 6.45 μm laser, have been developed, including chalcogenides and phosphorus compounds, such as $AgGaSe_2$ (AGSe) [6], $LiInS_2$ (LIS) [7], $LiInSe_2$ (LISe) [8], $BaGa_4S_7$ (BGS) [9], $BaGa_4Se_7$ (BGSe) [10,11], and $CdSiP_2$ (CSP) [12].

Among these NLO crystals, BGSe [13,14], is a potential NLO crystal for generating MIR radiation by parametric down-conversion. It is a new positive biaxial selenide compound and belongs to the *m* monoclinic point group, space group P_c, with *a* = 7.6252(15) Å, *b* = 6.5114(13) Å, *c* = 14.702(4) Å, *β* = 121.24°, and Z = 2. Moreover, BGSe crystal can operate under high pulse energy, owing to its excellent, intriguing characteristics. For example, firstly, it has high NLO coefficients with the two major nonlinear tensor elements of d_{16} = 31.5 and d_{23} = 22.1 pm/V [15]. Secondly, we should note that BGSe crystal can be processed in a large aperture via the Bridgman–Stockbarger method, which is favorable for high pulse energy operation. Besides, it has an intrinsic wide bandgap of about 2.73 eV, which can help to enhance the damage threshold (a surface laser damage threshold of 557 MW/cm² at 1 μm with 1 Hz and 5 ns is about 3.7 times that of $AgGaS_2$ [16]) and avert the nonlinear absorption effect (two-photon absorption, TPA) of economical 1 μm lasers [16,17]. Furthermore, theoretical modeling indicates that the chemical kinetics happen on the nanosecond (ns) time scale, guiding us to research ns pulsed 6.45 μm MIR lasers with high energy and narrow linewidths [2,18].

Several works on 6.45 μm ns MIR generation, from a 1 μm laser based on BGSe-OPO, were reported [19,20]. For example, a ns BGSe-OPO pumped by Q-switched $Nd:YLiF_4$ laser at 1053 nm was reported. MIR idler wave tuning from 2.6 to 10.4 μm was demonstrated with an angle-tuned, type-I (o → e + e) phase-matching *y*-cut sample, but the output energy at 6.45 μm was only about 13 μJ [19]. Moreover, widely tunable MIR radiation from 2.7 to 17 μm was demonstrated. Using a wide pump beam diameter (Φ = 5 mm) to accommodate the available high-energy from a diode-pumped Nd:YAG master oscillator power amplifier (MOPA) system (up to E_p = 250 mJ for 8 ns pulse at a repetition rate of 10 Hz), the maximum pulse energy of ~1 mJ at 6.45 μm with the pulse width of ~10 ns was obtained, but it gave a wide spectral FWHM of 9 nm at 7.2 μm [20]. Moreover, unfortunately, the MOPA pump system was very complex, bulky, and expensive, which limits its applicability.

In this paper, we report a compact, high pulse energy, and narrow linewidth MIR laser at 6.45 μm, from a BGSe-OPO system pumped by a 1.064 μm Nd:YAG oscillator. With an input energy of 58 mJ and repetition rate of 10 Hz, an output pulse energy of 1.23 mJ at 6.45 μm, pulse duration of 24.3 ns, and spectral FWHM of 6.8 nm were obtained for the first time, corresponding to an optical–optical conversion efficiency of ~2.1% from pump beam to idler beam. As far as we know, this is the highest pulse energy at 6.45 μm, with the narrowest linewidth for any all-solid-state MIR ns laser in BGSe-OPO pumped by a 1.064 μm oscillator. This laser has a simple design and compact structure, which is very suitable for tissue cutting.

2. BGSe Crystal Phase-Matching Characteristics

For the BGSe crystal, the phase-matching characteristics can be calculated by the following Sellmeier equations (S-E) [21]:

$$n_x^2 = 6.72431 + \frac{0.26375}{\lambda^2 - 0.04248} + \frac{602.97}{\lambda^2 - 749.87} \tag{1}$$

$$n_y^2 = 6.86603 + \frac{0.26816}{\lambda^2 - 0.04259} + \frac{682.97}{\lambda^2 - 781.78} \tag{2}$$

$$n_z^2 = 7.16709 + \frac{0.32681}{\lambda^2 - 0.06973} + \frac{731.86}{\lambda^2 - 790.16} \tag{3}$$
$$(0.901 \le \lambda \le 10.5910)$$

where λ is in micrometers. The phase-matching angles of BGSe-OPO pumped by 1.064 μm are shown in Figure 1a. It can be seen that the BGSe crystal can satisfy the type-I and type-II phase-matching conditions in the *x-z* and *y-z* principal planes. In the monoclinic class, *m* symmetry crystals, one of the principal dielectric axes (*xyz*), are always parallel with the *b* crystallographic axis. In our paper, for BGSe, it is $x \equiv b$, so the corresponding expressions for the effective nonlinearity coefficients of BGSe read [20]:

$$d_{eff-I}(x-z) = d_{16} \cos^2 \theta + d_{23} \sin^2 \theta \tag{4}$$

$$d_{eff-II}(x-z) = -d_{24} \sin \theta \tag{5}$$

in the *x-z* principal plane and

$$d_{eff-I}(y-z) = \pm d_{16} \cos \theta - d_{15} \sin \theta \tag{6}$$

$$d_{eff-II}(y-z) \approx 0 \tag{7}$$

in the *y-z* principal plane, where the tensor components d_{15}, d_{16}, d_{23}, and d_{24} can be found in [15]. Moreover, we take all the (θ, φ) on the phase-matching curves to calculate the d_{eff}, which are shown in Figure 1b. It was confirmed that the suitable phase-matching directions of the BGSe crystals are located in *x-z* and *y-z* principal planes. In Figure 1b, type-I phase-matched BGSe in the *x-z* principal plane and type-II phase-matched BGSe in *y-z* principal plane have approximative d_{eff}, but there was a wider accept angle and accept bandwidth in the *x-z* principal plane. Therefore, in our experiment, BGSe crystal was cut at $\theta = 47.1°$ and $\varphi = 0°$, whose d_{eff} is about twice that of AGS crystal (~15.8 pm/V).
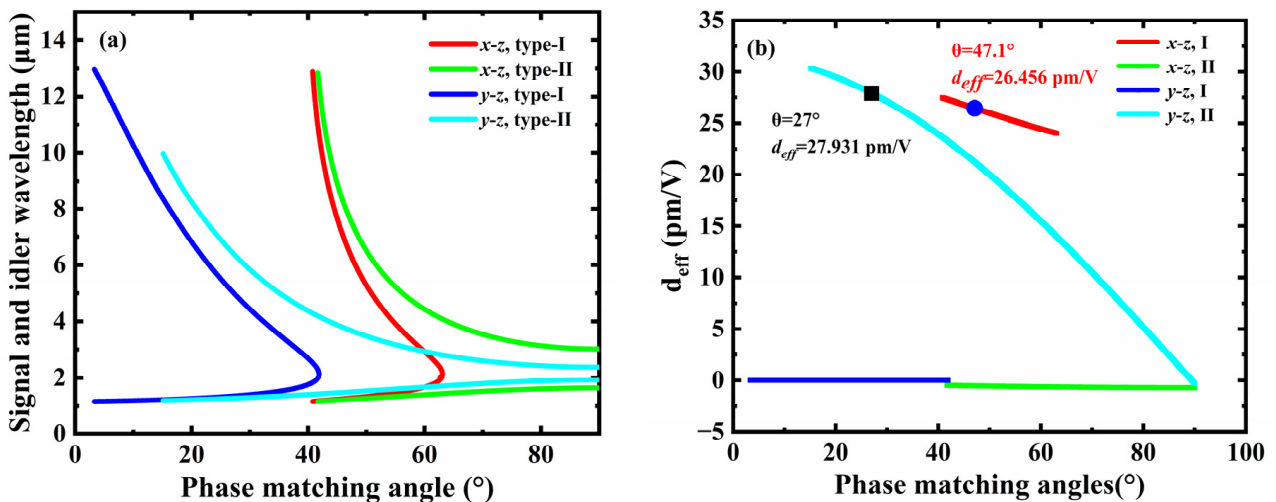

Figure 1. Calculated phase-matching characteristics of BGSe-OPO pumped by 1.064 μm laser. (**a**) Phase-matching angles versus OPO signal and idler wavelength at the *x-z* principal plane and *y-z* principal plane of BGSe crystal. (**b**) The OPO effective nonlinear optical coefficients d_{eff} versus phase-matching angles at the *x-z* and *y-z* principal planes.

3. Experimental Setup

The experimental configuration is shown in Figure 2. A linear cavity was adopted for BGSe-OPO. The pump source was an electro-optical (EO) Q-switched Nd:YAG oscillator at 1.064 μm at 10 Hz (LPS-1064-S-200 mJ). The maximum pulse energy was 200 mJ, with a pulse duration of 10 ns. Firstly, an optical isolator (ISO) was employed to avoid possible

damage to the pump source, as caused by the reflected pump light. Then, the incident light was reshaped and collimated by a telescope system (TS) to a Gaussian beam with a spot diameter of 2 mm. Next, an attenuator, which consisted of a half wave plate (HWP) and 45° polarized beam splitter (PBS) at 1064 nm, was utilized to adjust the incident energy at vertical polarization, without altering the pulse duration and pump beam profile. A large aperture $6 \times 6 \times 18$ mm^3 BGSe crystal was grown by the Bridgman-Stockbarger method. Both end facets of BGSe crystal were finely polished and coated with high transmittance (HT) via 1.064, 1.274, and 6.45 μm lasers. The transmission spectrum of the uncoated BGSe sample, in the range of 0.2~20 μm, is shown in the inset of Figure 2. It has better transmission in the range of 1~12 μm and can transmit up to 18 μm. The OPO cavity was constructed of two parallel-plane mirrors, i.e., M1 and M2, and the coating parameters were as follows: M1: 1.064 μm HT, 1.274 and 6.45 μm high reflectivity (HR); M2: 1.064 and 1.274 μm HR, 6.45 μm, with partial transmittance of 40%. The physical length of the cavity was about 25 mm. A germanium (Ge) wafer with a transmittance of 42% at 6.45 μm was placed behind the output coupling (OC) mirror, M2, in order to block the residual pump and signal waves. An energy meter was placed behind the Ge wafer to detect the energy of the idler laser.
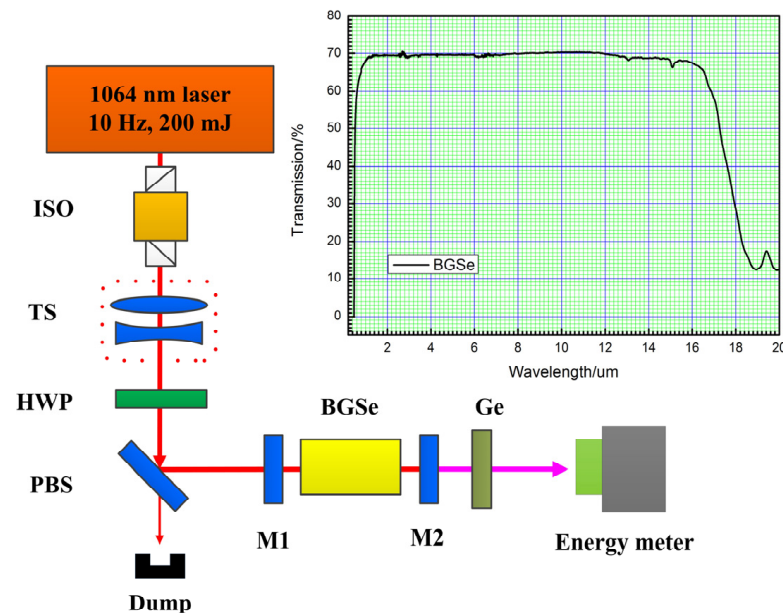
Figure 2. Schematic of the experimental setup. ISO: optical isolator; TS: telescope system; HWP: half-wave-plate at 1.064 μm; PBS: 45° polarized beam splitter at 1.064 μm; M1: input coupler (plane mirror); M2: output coupler (plane mirror); Ge: germanium filter mirror. Inset: transmission spectrum of uncoated BGSe sample in 0.2~20 μm range.

4. Results and Discussion

Firstly, a theoretical simulation model was established based on three-wave mixing equations to adjust the parameters of OPO. By supposing a pump beam with good Gaussian distribution in space and time and considering the effect of absorption and spatial birefringent walk-off in BGSe crystal, the relationship between the idler energy at 6.45 μm and input pump energy was simulated by the SNLO software, as well as plotted in Figure 3 with a black dashed curve. In the model, with the increase of the pump energy, there was no saturation phenomenon for the idler wave output energy.
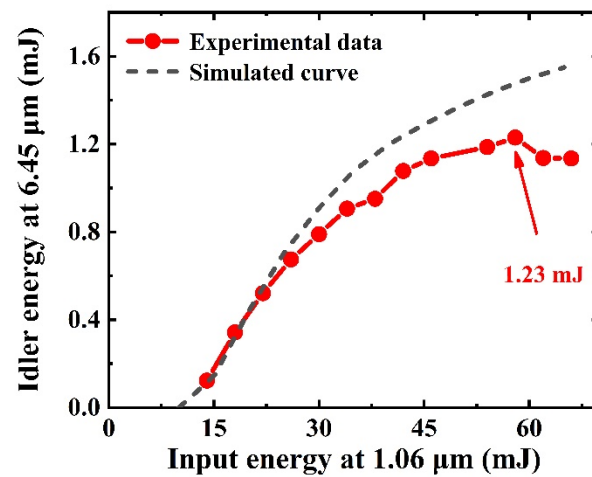
Figure 3. Output idler energy at 6.45 μm versus input energy in simulation and experiment.

With the above parameters, the experimental input-output characteristic is shown, as plotted in Figure 3 red solid circles (measured by an energy meter of OPHIR, PE10-C, metallic probe, with the maximum range of 10 mJ covering the wavelength range from 0.15 to 12 μm). The oscillator exhibits pump threshold energy as low as 10 mJ, which corresponds to the energy fluence of 0.318 J/cm^2. Then, the output pulse energy increases monotonically when the injected pump energy is below ~58 mJ; then, a rollover can be noticed, while the input pump energy exceeds ~58 mJ. A maximum pulse energy was up to 1.23 mJ at 6.45 μm under the pump energy of 58 mJ, corresponding to a peak power density of 60.7 MW/cm^2. The optical-optical conversion efficiency is 2.1%, from 1.064 to 6.45 μm. The pump pulse energy could not be improved further, as it was limited by the damage threshold of AR coating at BGSe crystal end facts (~80 MW/cm^2). It is observed in Figure 3 that the simulated results are in close agreement with the experimental data when the injected pump energy is below ~30 mJ. At higher pump energy, the experimental data are a little less than the numerical results, which may be attributed to ignoring the effect of the thermally-induced diffraction caused by BGSe crystal absorption in the simulation.

Similarly, the OPO optical-optical conversion efficiency, from 1.064 to 6.45 μm, versus BGSe crystal length at the fixed pump pulse energy of 58 mJ was calculated, as presented in Figure 4 (red curve). It can be seen in Figure 4 that the conversion efficiency increases with increasing BGSe crystal length to be ~9% around with a 22 mm long crystal. Then, the conversion efficiency falls off after a crystal longer than 22 mm, due to back conversion. The BGSe crystal we used was the only available crystal with a length of 18 mm. The experimental datum is also shown in the Figure 4. It is in close agreement with the simulated OPO conversion efficiency of 2.6%, which is similar to the conversion efficiency of ~3.3% in Ref. [20]. To confirm further the correctness of the simulation of optical-optical conversion efficiency, as a function of crystal length, the other experimental datum at the BGSe crystal length of 16.5 mm was added to Figure 4. The experimental optical-optical conversion efficiency is about 1%, close to the simulated value of 1.15%. Therefore, we think the simulation of optical-optical conversion efficiency, as a function of the crystal length, is credible. Although spatial birefringent walk-off in BGSe crystal was considered in simulation, the walk-off length was about 69 mm, assuming three waves with the same spot radii of 1 mm, which was much longer than the length of the crystal (18 mm) in our experiment. Therefore, the walk-off effect weakly influenced the conversion efficiency. In the following work, we enabled scale-up for the single pulse energy or conversion efficiency at 6.45 μm by choosing an optimum crystal length of about 22 mm, based on improving our crystal growth technique or optimizing the OC transmittance and thermal distribution in a shorter length BGSe crystal.
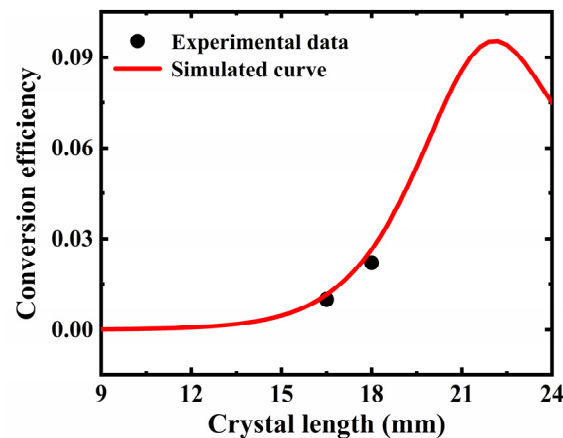
Figure 4. Simulated optical-optical conversion efficiency from 1.064 to 6.45 μm versus crystal length at mixed pump pulse energy of 58 mJ. The black dots represent the experimental data at the BGSe crystal lengths of 16.5 and 18 mm, respectively.

The pulse temporal profiles of pump and idler beams were measured via InGaAs (DET10A/M, THORLABS, rise time < 1 ns, 200~1100 nm) and HgCdTe (PDAVJ10, THOR-LABS, 2.0~10.6 μm, bandwidth 100 MHz) photo-detectors, respectively, which were simultaneously connected with 2 GHz bandwidth digital oscilloscopes (Tektronix, MSO 5204B, Beaverton, OR, USA). The measured typical oscilloscope traces are displayed in the Figure 5, under the input pulse energy of 58 mJ, suggesting the pump and idler pulse durations of 30.4 and 24.3 ns, respectively. The idler FWHM pulse duration was shorter than the incident pump pulse duration because of the temporal gain narrowing effect [22].
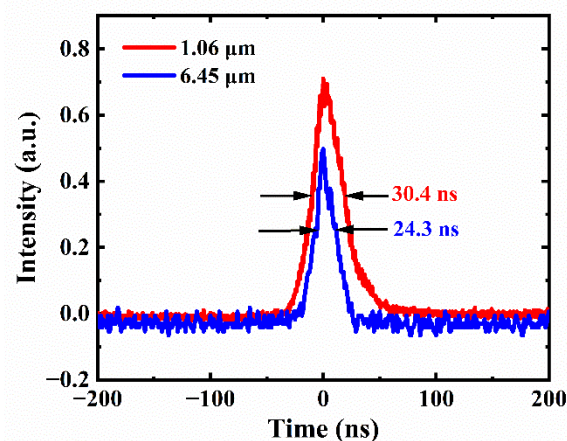
Figure 5. Measured temporal profiles of the incident pump and idler lasers.

The typical spectrum characterization of the pump wave was measured by optical spectrum analyzer (Ocean Optics, Dunedin, FL, USA, HR4000, resolution 0.02 nm, 200 nm~1100 nm). The measurement result is shown in the upper inset of Figure 6. The pump central wavelength is located at 1064.1 nm, with a spectral width of ~0.8 nm. Moreover, according to the OPO momentum conservation condition ($1/\lambda_p = 1/\lambda_s + 1/\lambda_i$) and phase-matching angle ($\theta = 47.1°$ and $\varphi = 0$) of BGSe, in this case, the signal wavelength λ_s and idler wavelength λ_i were calculated to be 1.274 and 6.45 μm, respectively. The linewidth of signal and idler light may be generated with a wide band of pump light and divergence angle of pump beam. In our experiment, the pump beam is collimated in BGSe crystal, so we focus on the effect of the pump beam linewidth on idler beam linewidth. When three waves are collinear in BGSe crystal, according to the conservation of momentum and

energy at type-I phase-matching, the coupling equations of the signal, idler, and pump lights can be written by:

$$\omega_p n_p^o = \omega_s n_s^e + \omega_i n_i^e \tag{8}$$

$$\Delta\omega_p = \Delta\omega_s + \Delta\omega_i \tag{9}$$

where n_j is the refractive index of the nonlinear crystal at angular frequency, ω_j for the pump, signal, or idler waves ($j = p, s, i$), and $\Delta\omega_j$ ($j = p, s, i$) represents the spectral FWHM of the pump, signal, and idler beams, respectively. The above two equations are combined, and the higher-order terms are ignored, so the idler linewidth is generated by the pump linewidth, as follows [23]:

$$\Delta\lambda_i = \left(\frac{n_{eff.p} - n_{eff.s}}{n_{eff.i} - n_{eff.s}}\right) \times \frac{\lambda_i^2}{\lambda_p^2} \times \Delta\lambda_p \tag{10}$$

where $n_{eff.j}$ ($j = p, s, i$) can be written as follows:

$$n_{eff.j} = n_j + \frac{\partial n_j}{\partial \omega_j}\omega_j \tag{11}$$
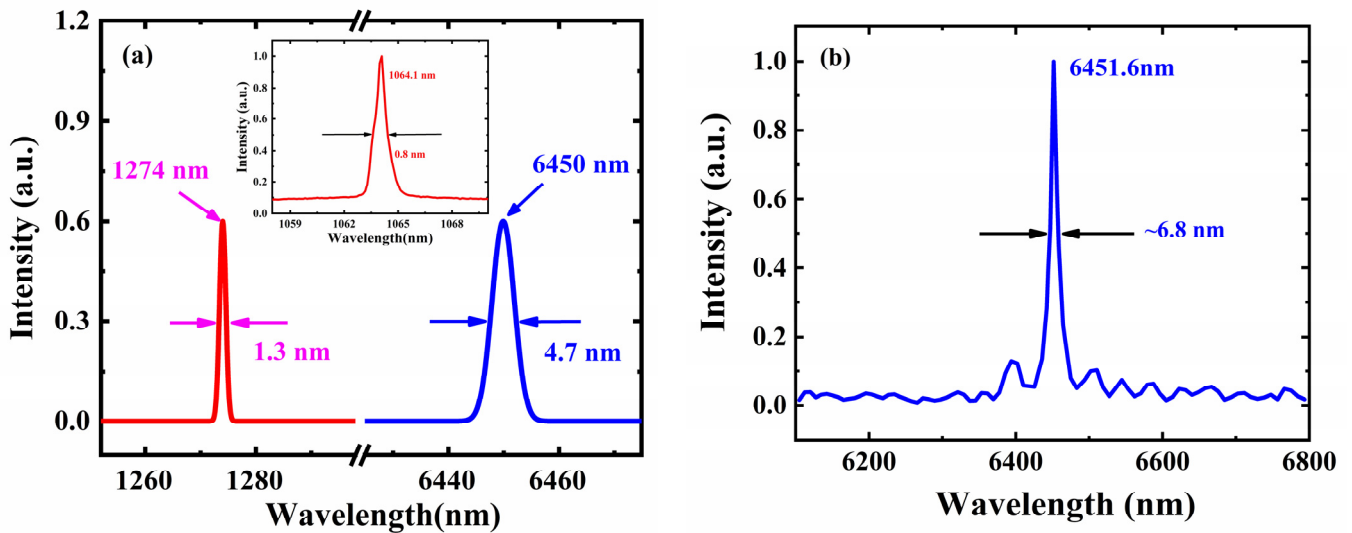
Figure 6. Measured and simulated spectra of the pump, signal, and idler beams in BGSe-OPO. (**a**) Simulation of signal and idler laser wavelength and linewidth. The inset at the top: the measured pump spectrum at 1064 nm. (**b**) Measured spectrum of output idler beam.

Further, assuming the pump, idler, and signal beams with a Gaussian spectral profile, the corresponding linewidths at 1.274 and 6.45 μm were estimated according to Equations (10) and (11) and shown in Figure 6a. It can be seen that the linewidth at 6.45 μm is about 4.7 nm. In addition, the exact emitted idler wavelength was monitored by a spectrometer (Arcoptix FT-IR 2-12, 0.4/cm, 2–12 μm, Arcoptix, Neuchatel, Switzerland). The typical result of an idler beam at 6451.6 nm is plotted in Figure 6b, with a corresponding spectral FWHM of ~6.8 nm, which is less than that in Ref. [20].

5. Conclusions

In conclusion, we have demonstrated a compact, high pulse energy, and narrow linewidth 6.45 μm laser, based on BGSe-OPO and pumped by a 1064 nm oscillator. A maximum output pulse energy of 1.23 mJ, with the linewidth of 6.8 nm was obtained, which is the highest energy with narrow linewidth at 6.45 μm, to the best of our knowledge. The pulse duration was measured to be about ~24.3 ns. Meanwhile, the output idler energy versus input pump energy and optical-optical conversion efficiency versus the BGSe length

were simulated. The calculated results were in close agreement with the experimental data. This 6.45 μm OPO system is precise and appropriate in applications. Such a high pulse energy can meet the tissue cutting threshold requirements (~1 mJ) [2]. In addition, pulses with narrow bandwidth are profitable for improving tissue ablation accuracy.

References

1. Edwards, G.S.; Austin, R.H.; Carroll, F.E.; Copeland, M.L.; Couprie, M.E.; Gabella, W.E.; Haglund, R.F.; Hooper, B.A.; Hutson, M.S.; Jansen, E.D.; et al. Free-electron-laser-based biophysical and biomedical instrumentation. *Rev. Sci. Instrum.* **2003**, *74*, 3207–3245. [CrossRef]
2. Edwards, G.S.; Pearlstein, R.D.; Copeland, M.L.; Hutson, M.S.; Latone, K.; Spiro, A.; Pasmanik, G. 6450 nm wavelength tissue ablation using a nanosecond laser based on difference frequency mixing and stimulated raman scattering. *Opt. Lett.* **2007**, *32*, 1426–1428. [CrossRef] [PubMed]
3. Edwards, G.; Logan, R.; Copeland, M.; Reinisch, L.; Davidson, J.; Johnson, B.; Maciunas, R.; Mendenhall, M.; Ossoff, R.; Tribble, J.; et al. Tissue ablation by a free-electron laser tuned to the amide II band. *Nature* **1994**, *371*, 416–419. [CrossRef] [PubMed]
4. Temelkov, K.A.; Vuchkov, N.K.; Freijo-Martin, I.; Lema, A.; Lyutov, L.; Sabotinov, N.V. Experimental study on the spectral and spatial characteristics of a high-power He-SrBr$_2$ laser. *J. Phys. D Appl. Phys.* **2009**, *42*, 115105. [CrossRef]
5. Tyazhev, A.; Kolker, D.; Marchev, G.; Badikov, V.; Badikov, D.; Shevyrdyaeva, G.; Panyutin, V.; Petrov, V. Midinfrared optical parametric oscillator based on the wide-bandgap BaGa$_4$S$_7$ nonlinear crystal. *Opt. Lett.* **2012**, *37*, 4146–4148. [CrossRef] [PubMed]
6. Boyko, A.A.; Marchev, G.M.; Petrov, V.; Pasiskevicius, V.; Kolker, D.B.; Zukauskas, A.; Kostyukova, N.Y. Intracavity-pumped, cascaded AgGaSe$_2$ optical parametric oscillator tunable up to 18 μm. *Opt. Express* **2015**, *23*, 33460–33465. [CrossRef]
7. Chen, W.; Poullet, E.; Burie, J.; Boucher, D.; Sigrist, M.W.; Zondy, J.J.; Isaenko, L.; Yèlisseyev, A.; Lobanov, S. Widely tunable continuous-wave mid-infrared radiation (5.5–11 μm) by difference-frequency generation in LiInS$_2$ crystal. *Appl. Opt.* **2005**, *44*, 4123–4129. [CrossRef]
8. Powers, P.E.; Tyazhev, A.; Marchev, G.; Vedenyapin, V.; Kolker, D.; Yelisseyev, A.; Lobanov, S.; Isaenko, L.; Zondy, J.-J.; Petrov, V. LiInSe$_2$ nanosecond optical parametric oscillator tunable from 4.7 to 8.7 μm. *Proc. SPIE* **2010**, *7582*, 75820.
9. Zhang, J.J.; Yang, F.; Yang, S.D.; Fang, S.H.; Wang, X.J.; Peng, Q.J.; Ye, N.; Xu, Z.Y. Tunable mid-IR optical parametric amplifier pumped at 1064 nm based on a wideband-gap BaGa$_4$S$_7$ crystal. *Infrared Phys. Technol.* **2020**, *111*, 103571. [CrossRef]
10. Yang, F.; Yao, J.Y.; Xu, H.Y.; Zhang, F.F.; Zhai, N.X.; Lin, Z.H.; Zong, N.; Peng, Q.J.; Zhang, J.Y.; Cui, D.-F.; et al. Midinfrared optical parametric amplifier with 6.4–11 μm range based on BaGa$_4$Se$_7$. *IEEE Photonics Technol. Lett.* **2015**, *27*, 1100–1103. [CrossRef]
11. Zhang, Y.; Zuo, Y.; Li, Z.; Wu, B.; Yao, J.; Shen, Y. High energy mid-infrared laser pulse output from a BaGa$_4$Se$_7$ crystal-based optical parametric oscillator. *Opt. Lett.* **2020**, *45*, 4595–4598. [CrossRef] [PubMed]
12. Chaitanya Kumar, S.; Zawilski, K.T.; Schunemann, P.G.; Ebrahim-Zadeh, M. High-repetition-rate, deep-infrared, picosecond optical parametric oscillator based on CdSiP$_2$. *Opt. Lett.* **2017**, *42*, 3606–3609. [CrossRef] [PubMed]
13. Yao, J.; Mei, D.; Bai, L.; Lin, Z.; Yin, W.; Fu, P.; Wu, Y. BaGa$_4$Se$_7$: A new congruent-melting IR nonlinear optical material. *Inorg. Chem.* **2010**, *49*, 9212–9216. [CrossRef] [PubMed]

14. Petrov, V.; Badikov, V.V.; Badikov, D.V.; Shevyrdyaeva, G.S.; Kato, K.; Miyata, K.; Mitin, K.V.; Wang, L.; Heiner, Z.; Panyutin, V. Barium nonlinear optical crystals for the mid-IR: Characterization and some applications. *J. Opt. Soc. Am. B* **2021**, *38*, B46–B58. [CrossRef]

15. Zhao, X.; Li, C.; Bai, J.; Wang, Z.; Yao, J.; Tan, R.; Xu, X. Recalibration of the nonlinear optical coefficients of BaGa$_4$Se$_7$ crystal using second-harmonic-generation method. *Opt. Lett.* **2021**, *46*, 5894–5897. [CrossRef]

16. Yao, J.Y.; Yin, W.L.; Feng, K.; Li, X.M.; Mei, D.J.; Lu, Q.M.; Ni, Y.B.; Zhang, Z.W.; Hu, Z.G.; Wu, Y.C. Growth and characterization of BaGa$_4$Se$_7$ crystal. *J. Cryst. Growth* **2012**, *346*, 1–4. [CrossRef]

17. Yelisseyev, A.P.; Lobanov, S.I.; Krinitsin, P.G.; Isaenko, L.I. The optical properties of the nonlinear crystal BaGa$_4$Se$_7$. *Opt. Mater.* **2020**, *99*, 109564. [CrossRef]

18. Hutson, M.S.; Hauger, S.A.; Edwards, G. Thermal diffusion and chemical kinetics in laminar biomaterial due to heating by a free-electron laser. *Phys. Rev. E* **2002**, *65*, 061906. [CrossRef]

19. Kolker, D.B.; Kostyukova, N.Y.; Boyko, A.A.; Badikov, V.V.; Badikov, D.V.; Shadrintseva, A.G.; Tretyakova, N.N.; Zenov, K.G.; Karapuzikov, A.A.; Zondy, J.J. Widely tunable (2.6–10.4 μm) BaGa$_4$Se$_7$ optical parametric oscillator pumped by a Q-switched Nd:YLiF$_4$ laser. *J. Phys. Commun.* **2018**, *2*, 035039. [CrossRef]

20. Kostyukova, N.Y.; Boyko, A.A.; Badikov, V.; Badikov, D.; Shevyrdyaeva, G.; Panyutin, V.; Marchev, G.M.; Kolker, D.B.; Petrov, V. Widely tunable in the mid-IR BaGa$_4$Se$_7$ optical parametric oscillator pumped at 1064 nm. *Opt. Lett.* **2016**, *41*, 3667–3670. [CrossRef]

21. Kato, K.; Miyata, K.; Petrov, V. Phase-matching properties of BaGa$_4$Se$_7$ for SHG and SFG in the 0.901–10.5910 μm range. *Appl. Opt.* **2017**, *56*, 2978–2981. [CrossRef] [PubMed]

22. Boyd, R.W. *Nonlinear Optics*; Academic Press: New York, NY, USA, 2003.

23. Cui, Y.; Dai, J.; Gong, Q.; Wang, L.; Men, Y.; Shen, Y.R. Linewidth analysis of KBe$_2$BO$_3$F$_2$ crystal optical parametric oscillator. *Proc. SPIE* **2007**, *6839*, 683912-1–683912-4.